

Continuous Closed-Loop 4-Degree-of-Freedom Holdable Haptic Guidance

Julie M. Walker  and Allison M. Okamura 

Abstract—Haptic guidance can be beneficial for aiding or training human users in many applications, such as teleoperation, rehabilitation, and navigation. Existing world-grounded haptic devices can provide effective multi-degree-of-freedom movement guidance. Wearable or holdable haptic devices can enable larger workspaces and unencumbered movement, but their use in guidance beyond one or two degrees of freedom has been limited. A holdable haptic device, called the Pantogripper, was previously presented in a study demonstrating its intuitive, directional guidance cues in four separate degrees of freedom. Here, using the same device, we present a controller for providing continuous closed-loop guidance for path following. In a human study, participants followed translation and rotation guidance from the device to successfully traverse three 3D paths with either no visual feedback or only a visual preview of the paths. Results indicate promise for holdable haptic devices to effectively provide high-degree-of-freedom movement guidance when visual guidance is unavailable or unsuitable.

Index Terms—Haptics and haptic interfaces, human factors and human-in-the-loop, medical robots and systems.

I. INTRODUCTION

PHYSICAL guidance using the sense of touch is a natural tool for training or assisting human movements in applications such as robotic teleoperation, navigation, and rehabilitation. Well-designed guidance through many sensory modalities can reduce cognitive load [1], such that guidance on certain aspects of a task enables the user to focus on a different aspect. Providing visual and auditory guidance through augmented reality (AR) during complex tasks has been shown to improve speed, performance, and effort [2].

Through touch, users can sense direction and magnitude in multiple dimensions and on multiple contact points on the body, making it suitable for movement guidance. Additionally, haptic information does not obscure simultaneous visual or audio information, and it can be unobtrusive and private. Many researchers have demonstrated benefits of haptic information in learning and

Manuscript received April 19, 2020; accepted August 10, 2020. Date of publication September 1, 2020; date of current version September 10, 2020. This letter was recommended for publication by Associate Editor E. Mazomenos and Editor P. Valdastri upon evaluation of the Reviewers' comments. This work was supported in part by the National Science Foundation Graduate Research Fellowship, in part by the Stanford Graduate Fellowship, in part by the National Science Foundation under Grant 1812966, in part by the Toyota Research Institute (TRI), and in part by the Human-centered AI seed grant program from the Stanford AI Lab, Stanford School of Medicine and Stanford Graduate School of Business. (Corresponding author: Julie M. Walker.)

The authors are with the Department of Mechanical Engineering, Stanford University, Stanford, CA 94305 USA (e-mail: juliewalker@alumni.stanford.edu; aokamura@stanford.edu).

Digital Object Identifier 10.1109/LRA.2020.3020581

performing physical tasks. Spreading information over multiple sensory channels helps reduce mental workload [3], and haptic cues can be easier to process than visual or auditory cues when attention is divided [4]. In physical tasks, touch guidance can improve learning [5], task performance [6], and rehabilitation [7]. It can be especially beneficial for motor learning in tasks where timing is a critical component [5], [8]. Some research has also shown learning benefits from haptic error augmentation, rather than assistance [9].

Forces applied to a user depend on equal and opposite reaction forces applied elsewhere. Most haptic displays used for high-dimensional haptic guidance have been large, world-grounded systems like consoles for robot-assisted surgery [10] that can apply reaction forces to an external surface. World-grounded systems are typically more expensive and bulkier than handheld or wearable haptic displays and have a limited workspace. Additionally, haptic guidance through a world-grounded system can cause instability in teleoperation control loops [10]. Wearable or holdable displays could enable haptic guidance throughout large, unencumbered workspaces for many applications, such as teleoperation, augmented reality, and medical training. Most ungrounded displays are unable to provide true kinesthetic forces and torques onto a user's hand or body because they lack external grounding. Few exist that provide directional haptic cues in more than one or two degrees of freedom (DOF). As such, there has been little research to understand ungrounded haptic guidance for high-DOF movement tasks.

In this letter, we present a closed-loop controller for position guidance from a 4-DOF holdable haptic device in a path following task. This haptic device, called the Pantogripper (Fig. 1), was presented in [11]. Users' responses to simple open-loop cues varied in magnitude and speed, motivating the use of closed-loop guidance. We validated the closed-loop controller in a study in which users followed continuous, closed-loop haptic guidance from the device with some or no visual information about the desired path. Results demonstrated that high-DOF holdable haptic guidance can help users perform correct motions when visual information is not available or would be obtrusive.

II. RELATED WORK

A. World-Grounded Haptic Guidance

Most haptic guidance research has been completed with traditional kinesthetic, world-grounded haptic devices, which can apply net forces and torques in multiple DOFs, making movement guidance relatively easy to provide. Through the use

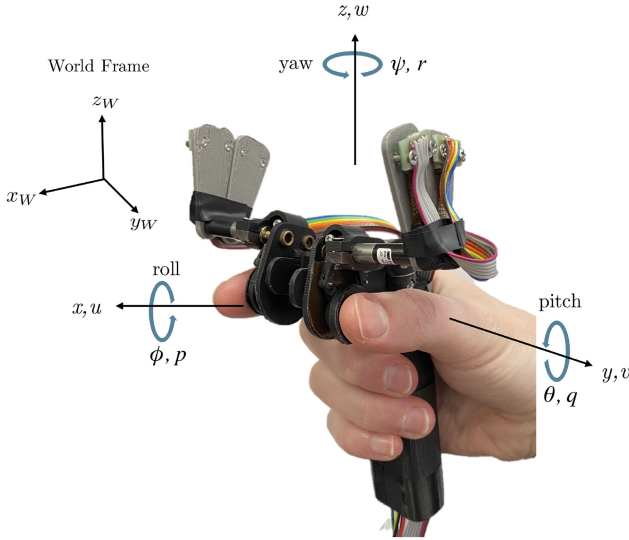


Fig. 1. The Pantogripper, shown with reference frames used for recording and analyzing motions.

of “Virtual fixtures,” a device can provide physical resistance to users manipulating a robot into certain regions of the workspace. Virtual fixtures are often implemented with proportional or proportional-derivative controllers for force-feedback, simulating virtual walls, although more complex controllers have been developed to avoid energy storage and potential instability [10], [12]. World-grounded kinesthetic devices have also been used to actively guide users’ hands toward target positions or through desired trajectories, which is relevant for motor learning, rehabilitation, and robotic shared control [12], [13].

B. Wearable and Holdable Haptic Guidance

Wearable and holdable haptic devices can be mobile, lightweight, and inexpensive, making them a desirable form for tasks that require large workspaces, portability, or free motion. In navigation, several ungrounded “haptic compasses” have been developed for planar guidance while walking. They change shape or weight distribution [14], [15] or use gyroscopic effects to generate distinct directional cues [16]. These ungrounded holdable methods may be capable of more complex guidance [17], but they must overcome limitations such as saturation, weight, and size.

Vibrotactile displays are common for guidance [18]–[21]. For a display to provide directional information through vibration, users must learn to interpret different vibration patterns [18], or vibrating actuators need to be spread out in space around the user’s body or hand [19]. One notable exception is through asymmetric vibrations, which generate a pulling sensation from a wearable or holdable device, but depend on consistent contact with a user’s skin [21].

Skin deformation, which is directional, is more intuitive than vibrotactile stimulation for motion guidance [22]. It has been applied successfully in wearable fingertip devices and holdable devices for sensory substitution in virtual reality and teleoperation [23]. For example, planar motion guidance through fingertip skin stretch has enabled users to match simple trajectories

within an average of 12 mm [24]. Wrist and arm-mounted skin deformation devices have also shown promise for providing movement guidance [25]. Guinan et al. developed a holdable aperture-grounded skin deformation device that generates guidance cues in 5-DOF by moving two tactors either in the same or opposite directions [26], and this technique inspired the device used in this letter. Prior work has included only individual target hand rotations and translations and has not used closed-loop guidance simultaneously in more than two DOFs.

III. GUIDANCE DEVICE AND CONTROL

The Pantogripper, presented in [11] and shown in Fig. 1, uses two 5-bar linkage pantograph mechanisms (one at each fingertip) to provide directional forces to the users’ fingerpads. The reference frames shown in Fig. 1 will be used throughout this letter. A guidance control algorithm displaces the pantograph end effectors proportionally to the user’s translation and rotation error, simulating a combined spring force and torque toward the correct pose at the nearest point on the path.

A. Device Design

Each pantograph can translate in any combination of x and z directions. As the end effectors move, they stretch the skin and displace the fingers, producing a salient directional pull. (The Weber Fraction for tangential skin stretch at the fingerpad is 0.15–0.20 [27].) By applying tangential cues in the same direction on each finger, the Pantogripper can generate cues to translate in the device’s x - z plane. By applying tangential cues in opposite directions on each finger, it generates a torque sensation, cuing the user to twist (yaw, ψ) or tilt left/right (roll, ϕ). In total, it can provide 4-DOF guidance. The reaction forces simultaneously applied at the handle are distributed over the palm and therefore are not noticeable, so the user feels almost as if an object held in a precision grip is being pulled or rotated by an external force.

Each pantograph has 10 mm-long upper links and 13 mm-long lower links. The forward and inverse kinematic equations are given in [28]. The links and all mountings are 3D printed rigid polyurethane. Metal pins connect each joint, and a circular pad rotates freely on the bottom pin. Faulhaber coreless micro DC motors (64:1 gear ratio) with optical encoders (50 counts/rev) power each upper joint. The end effectors have nylon on their inner surfaces so that they slide smoothly against a vertical support. The link lengths and motors were selected to provide similar workspace and force output to a previous fingertip device [29]. A high-friction rubber material on the outer surfaces of the end effectors prevents slip between each end effector and the users’ finger pad. A motor and capstan transmission at the gripping hinge produces a small constant outward force to maintain contact with the user’s fingers. The arms adjust to accommodate fingers of different lengths. The device weighs 76 g. An Ascension trakSTAR 6-DOF magnetic tracking system (Northern Digital Inc., Waterloo, Ontario, Canada) records the device’s position and orientation at 80 Hz. A magnetic sensor is mounted in the bottom of the handle. This location was chosen

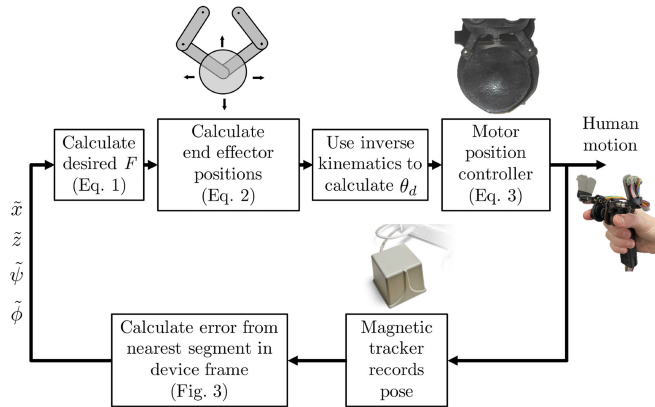


Fig. 2. The control and feedback system operating the Pantogripper for continuous guidance.

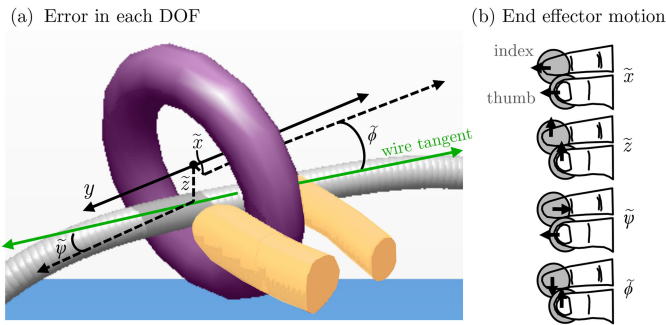


Fig. 3. (a) Ring on wire task, where the ring is held by the thumb and index finger: Translation errors \tilde{x} and \tilde{z} and rotation errors $\tilde{\psi}$ and $\tilde{\phi}$ were calculated in the device reference frame between the ring center point and the closest point on the path. (b) Direction of end effector motion for errors in each DOF.

to prevent the magnets in the motors from affecting the tracking quality, which was checked using Ascension's proprietary software.

A Sensoray 826 PCI card handles the analog and digital I/O (Sensoray, Tigard, OR, USA). Custom linear current amplifiers (LM675 T, 0.1A/V gain) and a 13 V external power supply (Mouser Electronics Inc., Mansfield, TX, USA) power the motors. A C++ program runs the haptic controller at 1000 Hz and displays a virtual environment using the CHAI 3D simulation framework [30].

B. Guidance Controller

Fig. 2 shows the Pantogripper's continuous guidance control loop. The displacement of the two pantograph end effectors was commanded according to the user's current displacement from the desired pose. In our model, the user is the plant of the control loop. They sense the fingertip displacement and respond by translating and rotating their hand in the direction they feel pulled, ideally reducing the error. This study was based on a ring on wire task, commonly used in training for laparoscopic and robot-assisted surgery. This task is particularly suitable because the relevant DOF are the ones the Pantogripper provides. No guidance is necessary along the wire tangent (the device's y axis) or for rotation about the wire tangent (pitch, θ). Fig. 3

shows how errors are calculated in each of the device's four DOFs. The translation errors \tilde{x} and \tilde{z} were the difference from the ring's center point to the nearest point on the path, defined in the Pantogripper's reference frame shown in Fig. 1. The rotation errors $\tilde{\psi}$ and $\tilde{\phi}$ were calculated as the horizontal and vertical angles between the Pantogripper's y axis and the tangent to the path at the closest point. The guidance forces commanded to the user's fingertips were proportional to the error, as they are for many applications of virtual fixtures and active guidance with world-grounded haptic interfaces [12]:

$$\begin{aligned} F_x^{\text{index}} &= K_{\text{trans}} \tilde{x} + K_{\text{rot}} \tilde{\psi} \\ F_z^{\text{index}} &= K_{\text{trans}} \tilde{z} + K_{\text{rot}} \tilde{\phi} \\ F_x^{\text{thumb}} &= K_{\text{trans}} \tilde{x} - K_{\text{rot}} \tilde{\psi} \\ F_z^{\text{thumb}} &= K_{\text{trans}} \tilde{z} - K_{\text{rot}} \tilde{\phi}, \end{aligned} \quad (1)$$

where $K_{\text{trans}} = 350 \text{ N/m}$ and $K_{\text{rot}} = 7 \text{ N/rad}$ are the gains on the translation and rotation errors respectively. If the error was purely in translation, the end effectors would move in the same direction. If the error was purely in rotation, the end effectors would move in equal and opposite directions. The gains were tuned in pilot testing so that the end effector motion would be salient for small deviations from the path for pure translation, pure rotation, and their combination.

The pantograph end effectors are position controlled. We estimate that there is a linear position-force relationship using the average tangential skin displacement stiffness value found in [31], $k_{\text{skin}} = 1.58 \text{ N/mm}$. Each pantograph end effector's displacement from its center point, using the same reference frame as in Fig. 1, is

$$\begin{bmatrix} x \\ z \end{bmatrix}_P = \begin{bmatrix} F_x \\ k_{\text{skin}} \end{bmatrix}^T. \quad (2)$$

Thus, when there is no translation or rotation error from the path, the pantograph end effectors rest at the center of their workspace. The displacement was restricted to 3 mm in any direction to keep the pantograph end effector in a well-conditioned region of the workspace, presented in [11]. This corresponds to a maximum of 13.5 mm of translation error or 38.8° of rotation error. This range is comparable to a physical ring-on-the-wire laparoscopic training task. The ring from the Wire Chaser task (3-Dmed, Franklin, OH, USA) has an inner diameter of 13.7 mm. Fig. 4 shows an example of commanded outputs corresponding to errors in each direction. When $\tilde{\phi}$ is large in Fig. 4(b), the end-effectors are saturated in Fig. 4(d). The thumb end effector is fully downward and the index end effector is fully upward, cuing wrist pronation. The desired motor positions θ_d are calculated using the inverse kinematics given by [28]. The motor positions θ are current-controlled using a proportional-derivative controller:

$$i = \frac{k_p \tilde{\theta} + k_d \dot{\tilde{\theta}}}{N k_t}, \quad (3)$$

where i is the current commanded, $\tilde{\theta}$ is the motor angle error ($\theta - \theta_d$), the gains are $k_p = 5.5 \text{ Nm/rad}$ and $k_d = 0.004 \text{ Nms/rad}$, the gear ratio is $N = 64:1$, and the torque constant is $k_t =$

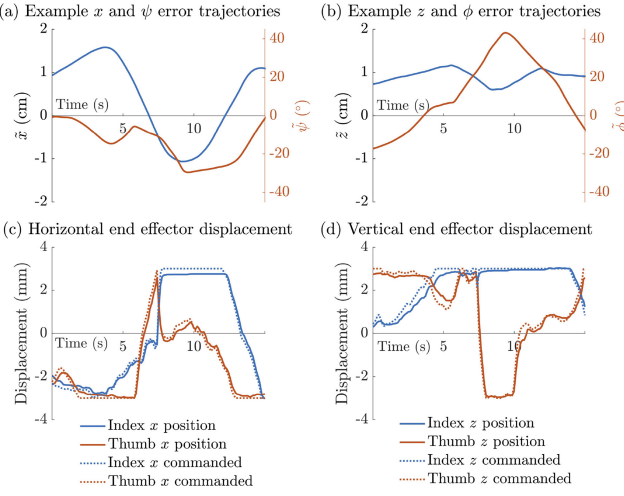


Fig. 4. (a) Example trajectory of errors in x and ψ and (c) corresponding commanded and actual end-effector motions in the horizontal direction. (b) Example trajectory of errors in z and ϕ and (d) corresponding commanded and actual end-effector motions in the vertical direction.

0.00196 Nm/A. The motor controller gains were tuned to eliminate perceivable noise while maintaining good position tracking at frequencies of volitional human motion, generally less than 10 Hz [32]. Fig. 4(b) and (d) show that the measured end effector positions closely track the commanded positions. The relationship in Eq. 2 is a simplification of the finger-pantograph interactions because the users' fingers are generally both displaced and stretched. The skin-deformation stiffness values in [31] were measured for a finger fixed in place. The magnitude of the force felt by the user depends on their grip force against the pads, finger impedance, and skin stiffness. These effects, as well as differences between users' perception and responsiveness, create uncertainty in the plant model of the control loop, further motivating closed-loop feedback for haptic guidance.

IV. EXPERIMENTAL METHODS

In a user study, 12 participants were asked to move their hands along curved 3D paths, as if manipulating a virtual ring along a wire, relying on haptic information – either with no vision of the path or only a preview of the path. Vision was limited in order to understand the role that haptic guidance could provide, independent of visual information. Additionally, haptic guidance might be particularly relevant in applications where visual information cannot be provided due to occlusion or visual overload. Participants were aged 22 to 32, and included five men and seven women. 11 participants were right-handed, and one was left-handed, to reveal any performance differences due to handedness. Seven participants were experienced with haptics experiments, and five participants had never participated in a haptics experiment before. The goal of this study was to understand whether guidance information from a handheld device could be used in closed-loop to help a user navigate a target path. Six additional participants completed the study with only a visual preview and no haptic guidance. These participants were right-handed, in the same age range, and experienced with

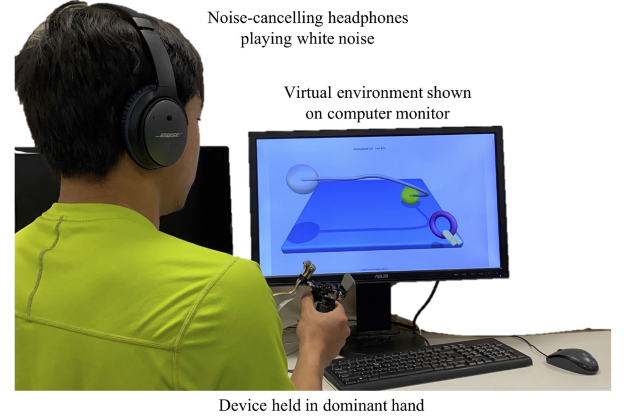


Fig. 5. Experimental setup. Users stood at a desk, holding the Pantogripper in their dominant hand and viewing a virtual environment on a computer screen.

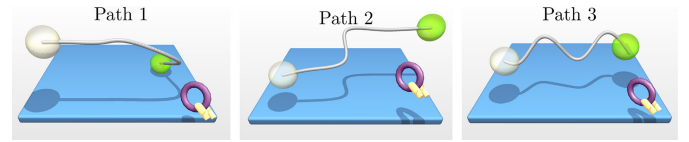


Fig. 6. Three paths: users traversed from the right to the left, as if moving the ring along the path without touching it. The path was not visible during any of the trials, but it was shown as a preview before trials in some conditions.

haptic experiments. The protocol was approved by the Stanford University Institutional Review Board, and the subjects gave informed consent (IRB protocol 22514).

Users stood at a desk, holding the Pantogripper in their dominant hand (Fig. 5). On a computer monitor, they saw a virtual environment (rendered in CHAI 3D [30]). The user's fingers were shown holding a ring, which was fixed to the virtual fingers in the same pose for all trials and could not be dropped. Because the environment was shown on a standard monitor rather than with a head-mounted display, the visual depth information was limited, but the shadows depicted in the scene helped users to discern depth.

Users completed two blocks of 12 trials. In one block, the *Preview and Haptics* condition, they were shown the path for each trial at the start of that trial (one of three paths, shown in Fig. 6). When they touched the start point, the green sphere on the right end of the path, the path disappeared. Additionally, the start point turned white, and the end point turned green, indicating that it was the new goal. While they moved from the start to the end, they received haptic guidance toward the closest position and orientation of the path, explained in Section III-B. In the other block, the *Haptics Only* condition, users were never shown the path and saw only the start and end points. They relied only on haptic guidance as they moved between the two blocks. Users were told the order they would complete the two blocks. They were instructed to prioritize accuracy over speed. After each block, they completed a survey based on the NASA Task Load Index rating their performance and effort.

TABLE I

MEAN μ AND STANDARD DEVIATION σ FOR TRIAL TIME, MEAN OVERALL AND MEAN MINIMUM EUCLIDEAN DISTANCES BETWEEN THE TIME-WARPED TRAJECTORIES AND DESIRED PATHS, AND RMS ERRORS IN EACH DEGREE OF FREEDOM

Condition		time (s)	mean dist (cm)	min dist (cm)	\tilde{x} (cm)	\tilde{z} (cm)	$\tilde{\psi}$ ($^{\circ}$)	$\tilde{\phi}$ ($^{\circ}$)
Haptics Only (n = 12)	μ	39.6	1.66	1.33	1.43	1.03	23.4	24.4
	σ	22.0	0.64	0.43	0.90	0.45	9.34	12.2
Preview and Haptics (n = 12)	μ	36.5	1.44	1.19	1.36	0.99	18.9	20.0
	σ	21.8	0.58	0.43	0.79	0.42	6.36	9.34
Preview Only (n = 6)	μ	12.6	1.34	1.30	1.18	0.92	18.4	15.5
	σ	5.38	0.42	0.42	0.58	0.47	8.59	6.93

The order of the two blocks was alternated between subjects. Three paths were repeated pseudorandomly throughout the experiment, such that each path was presented four times in each block. All of the paths were within a 20 cm \times 20 cm \times 20 cm region. The three paths were designed to require movement in each of the four DOF provided by the Pantogripper, to require simultaneous changes in two or more DOF, to be reasonably achievable without vision, and to avoid uncomfortable wrist poses. Path 3 approximates a path from 3-Dmed's Wire Chaser laparoscopic training task. Users completed 12 training trials with simpler paths before beginning the experiment. In the first four trials, the path was visible. In the next four trials, the path was shown before the trial began. In the last four trials, the path was never shown.

In order to understand the contribution of the path previews to performance, a different group of participants was asked to complete the same set of paths with no haptic guidance. Again, they saw a preview of the path, but it disappeared when they began each trial. Because this study was completed in a separate sitting, each user participant completed four training trials in which they followed simple paths with full vision and four training trials in which they saw only a preview of the path.

V. RESULTS

Performance was analyzed using four metrics: (1) Trial time, (2) Euclidean distance between desired paths and user trajectories after Dynamic Time Warping, (3) Mean minimum Euclidean distance reached to each point along the paths, and (4) Error in each DOF: x , z , ψ , and ϕ .

Metric 2 applies Dynamic Time Warping (DTW), which matches each time step in the user trajectories to each point on the paths such that the sum of the Euclidean distance errors for all the points is minimized. DTW error quantifies the correctness of the overall trajectory shape [33]. The mean DTW error may be skewed if the user pauses in a pose with high error. Metric 3 attempts to account for this by analyzing the minimum distance reached from each point along the path – how successful the users were at hitting each point. We believe this encodes users' ability to respond to haptic guidance provided during instances of high error by moving toward the correct pose. The last metric is the root-mean-square (RMS) error in the x , z , ψ , and ϕ directions from the nearest point on the path. This is the error calculation used for the guidance control algorithm, so it also represents the amount of haptic guidance a user experienced.

Table I lists the mean and standard deviation of these results for each condition.

For the *Haptics Only* and *Preview and Haptics* conditions, a multi-way Analysis of Variance (ANOVA) was completed for each metric for the independent variables condition, condition-order, path, and subject (as a random variable), followed by post-hoc multiple comparisons tests with Bonferroni corrections. The *Preview Only* condition was completed separately by a different set of subjects, so it was not included in the main analyses. However, a multi-way ANOVA was completed for all three conditions comparing metrics 1, 2, and 3 for the independent variables condition and path. Fig. 7 shows the mean and standard deviation of these metrics for each condition.

The mean warped Euclidean distance, minimum Euclidean distance, and RMS error from the desired paths for each DOF are shown in Table I. Users were able to follow the paths with mean distance of 1.66 cm, even with no view of the path and only haptic guidance. Fig. 8 shows recorded trajectories for the *Haptics Only* condition. Between the two haptic conditions, there was a significant difference in rotation RMS error. The *Preview and Haptics* condition had 4.5° lower ψ errors and 4.4° lower ϕ errors than the *Haptics Only* condition. There was not a significant difference in x and z errors. The path also had a significant effect on rotation errors, with Path 1 having significantly lower RMS $\tilde{\psi}$ than both other paths ($p < 0.05$). All three paths had significantly different RMS $\tilde{\phi}$: Path 2 errors were 11.06° higher than Path 1, and Path 3 errors were 12.95° higher than Path 2 ($p < 0.001$). There was no significant effect of block order, no significant difference was seen in the movements of the left-handed subject who completed the study, and there were no significant differences between survey responses between the two conditions.

Trials in the *Preview Only* condition were significantly shorter ($p < 0.001$), as seen in Fig. 7(a). There was no significant difference between the *Haptics Only* and *Preview and Haptics* conditions. For the combined *Haptics Only* and the *Preview and Haptics* Conditions, the mean time spent near each point on the path is depicted in Fig. 9. Users sometimes spent time seeking out haptic guidance by making small movements when they were unsure, as seen in several trajectories in Fig. 8 and in the longer time spent near the paths' bends in Fig. 9. The mean DTW Euclidean distance to the path was significantly larger in the *Haptics Only* condition than the other conditions ($p < 0.01$ for *Preview and Haptics* and $p < 0.001$ for *Preview Only*), as seen in Fig. 7(b). The mean minimum distance to the path was lowest in the *Preview and Haptics* condition, as seen in Fig. 7(c).

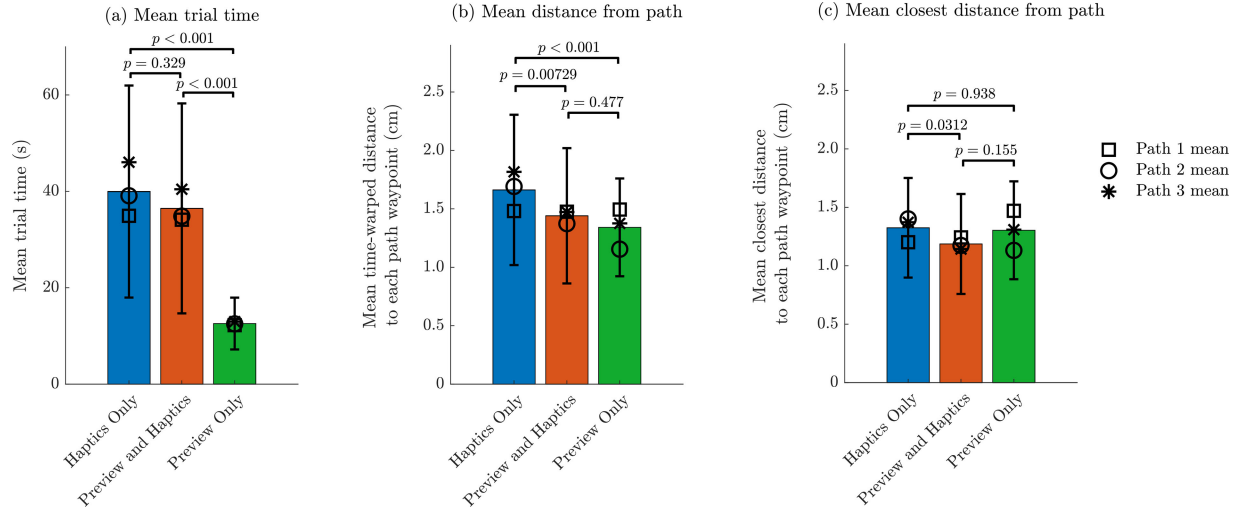


Fig. 7. (a) Mean and standard deviation of trial time for each condition. (b) The mean and standard deviation of the DTW Euclidean distance from the path for each condition. (c) The mean and standard deviation of the minimum distance reached to each point on the paths for each condition. (*Haptics Only* n = 12, *Preview and Haptics* n = 12, *Preview Only* n = 6)

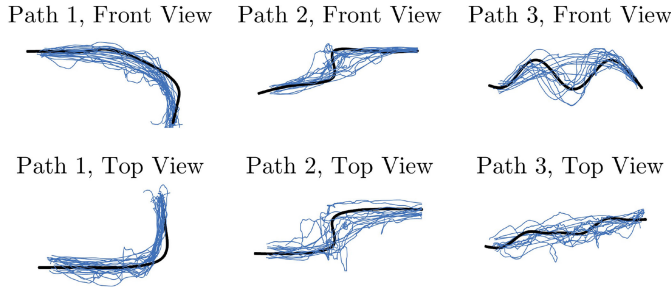


Fig. 8. Trajectories in the *Haptics Only* Condition

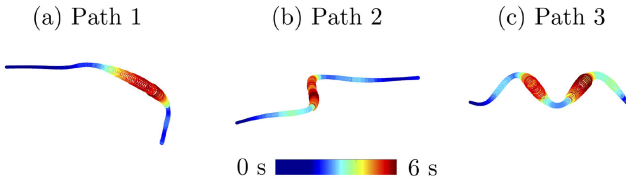


Fig. 9. Time spent along each of the three paths for conditions *Haptics Only* and *Preview and Haptics*.

Improvement over the *Haptics Only* condition was significant at the 0.05 level ($p = 0.0312$), but improvement over the *Preview Only* condition was not ($p = 0.155$).

VI. DISCUSSION

Proportional closed-loop haptic guidance from a holdable device can successfully guide users along unseen paths. Even without visual previews of the paths, users were able to follow the guidance, with mean DTW error below 1.7cm, and with mean rotational errors below 25° , given in Table I and Fig. 7. This performance is comparable to lower-DOF haptic guidance studies. In [24], users matched simple planar trajectories with an average of 1.2 cm error. In [34], mean error responding to wrist rotation cues was 23.2° .

This demonstrates that higher DOF hand-grounded haptic guidance can be effective, but there are opportunities for improvement. For Path 3, guidance to roll the hand and curve downward was not always effective, and users missed the dip in the middle of the path. With this controller, a vertical displacement error above 1.3 cm saturates the pantograph end effectors, obscuring roll cues unless the roll error grows very large. Additionally, once the end effectors are saturated, there is no additional movement, so users might lose track of the center position and interpret the device's inactivity as an indication they are in the correct position. This could be especially problematic if the user adjusted their grip during use, resetting their origin position. These limitations could be accounted for in future controllers by changing the gain tuning or using a nonlinear gain. Alternatively, the device could provide a cue that helps the user feel when the end effectors are at the zero-position, or notifies the user that the end effectors are saturated.

A. Strategies and Performance Differed by Condition

Differences in available haptic information and task criteria often change the strategies users take to complete haptic tasks [35]. In this study, strategies differed in the *Haptics Only* condition, *Preview and Haptics* condition, and *Preview Only* condition. The trajectories in Fig. 8 show that some users moved in a saw-tooth pattern or oscillated back and forth over certain parts of the path to seek out large displacements from the end effectors. Additionally, Fig. 9 shows that for the haptic conditions, participants paused in places with more curvature, trying to interpret haptic guidance, or they moved their hands around seeking out additional haptic information. Such strategies contributed to the significant increase in trial time between the haptics conditions and the *Preview Only* condition shown in Fig. 7(a) and Table I. In the *Preview Only* condition, participants tended to spend more time before each trial, studying the shape of the path, because they knew they would not have any way of gaining additional information during the trial. In both haptic

conditions, they instead spent time during the trial apparently seeking out virtual fixtures. This suggests that a controller with a deadband near zero and then a stiffer virtual wall might be more effective for this task. Although intended for world-grounded devices, several kinds of resistive and assistive fixtures discussed in [10] and [12] might be effective for holdable devices as well.

Overall, the *Preview Only* condition had the lowest mean Euclidean distance from the path, as shown in Fig. 7(b). In this task, vision was the most helpful source of information, even as just a preview before beginning each trial. Faster trial times in the *Preview Only* condition may also mean that participants were less likely to forget the path shape throughout the trial. Future studies should standardize the amount of time that a preview is provided or randomize the feedback condition in each trial to better understand the role of the visual preview. The *Haptics Only* condition had a significantly higher mean Euclidean distance error, listed in Table I and shown in Fig. 7(b). However, the error is only about 0.2 cm larger than the mean errors of the other conditions. Thus, the haptic feedback alone is capable of providing useful guidance for path following.

When considering the minimum distance reached for each waypoint along the path, the mean error is lowest for the *Preview and Haptics* condition (Fig. 7(c)). Although not significant at the 0.05 level, there is a notable improvement over the *Preview Only* condition (0.11cm, $p = 0.155$), which is hidden when comparing only the mean Euclidean distances (Fig. 7(b)). Participants were able to seek out and use the additional guidance provided by the haptic device to correct their error from the path. In contrast, in the *Preview Only* condition, they had to rely only on their memory of the path. This difference in strategy led to higher average error from the path when using haptic guidance, but participants may have been able to more closely align with each path point. The mean minimum distance reached in the *Haptics Only* and *Preview Only* conditions were not significantly different from each other, but combining the two guidance modalities slightly outperformed either independently. Further studies are necessary to understand this improvement, and changes to the controller design as discussed above might be able to improve the performance further or minimize the need for users to actively search for haptic information.

B. Directional Differences With Haptic Guidance

The *Preview and Haptics* and *Haptics Only* conditions were completed with the same set of subjects, so we are able to compare these conditions more directly. For both the *Haptics Only* and *Preview and Haptics* conditions, there were higher RMS errors in the x than the z direction in the device's reference frame. This might be due to differences in touch perception in different directions in the finger joints and fingertip skin [36]. In this controller, the gains for x and z errors were the same, but a more advanced controller might tune the gains based on these differences.

Rotation errors (both $\tilde{\psi}$ and $\tilde{\phi}$) were lower in the *Preview and Haptics* condition. This could indicate that the controller does not provide sufficient rotation information, and users benefited from extra visual information. The rotation guidance, as

discussed previously, may have been obscured by translation guidance when translation errors were large enough to saturate the pantograph end effector position. This could be addressed by increasing the controller gain for rotational errors relative to the translation error gain. Additionally, users in our study may have prioritized translation errors in the *Haptics Only* condition.

Although the responses to rotation cues in the previous Pantogripper study in [11] were very consistent, and participants in that study mentioned that they felt the rotation cues were the easiest to interpret, it is possible rotation cues were more confusing to users when the four DOFs were combined in this study. Understanding how many simultaneous DOFs users can easily respond to from holdable haptic displays such as this one could be helpful for designing better guidance controllers. Most guidance studies have been limited to one or two simultaneous DOFs. Using a controller that applies rotation and translation cues sequentially might make it easier for users to understand and respond to guidance.

There is substantial uncertainty in the force applied to the fingertips from the Pantogripper. Our controller estimated the force through Eq. 2, but it is affected by finger impedance, anisotropies and nonlinearities in skin stiffness, and the user's grip force on the handle and against the pantograph end effectors. By including force sensors in the end effectors in future designs, force control could be implemented instead of position control. Then the device could provide more consistent guidance forces in all instances and more closely mimic guidance provided by world-grounded haptic displays.

VII. CONCLUSION

Haptic guidance in 4 DOFs from a holdable device shows promise for guiding continuous movements. This device used a proportional control scheme to provide combined translation and rotation guidance toward the nearest segment of a path. Users successfully followed unseen paths using haptic guidance alone, or with a visual preview. Previews improved overall errors from the path, but in situations where visual guidance is inconvenient, overwhelming, or cannot be provided, multi-DOF haptic guidance could be effective even from devices unable to provide net forces and torques.

Other controllers should be considered to account for saturation, such as nonlinear mapping functions between error and guidance or pulsing patterns as in [24], [26], and [31]. However, delays responding to pulsing cues in [26] could make closed-loop control more challenging. In [11], there was a small delay in user responses to Pantogripper guidance cues, which is not addressed by this controller design. Future iterations, whether using sustained or pulsed cues, could benefit from modeling this delay. Future work should analyze performance and strategies in more complicated paths, dynamic trajectory following, and additional dexterous tasks such as placing a peg into a hole or suturing. Comparisons should be made between fully cutaneous, hand-grounded, and world-grounded haptic guidance in high-dimensional movements. Additionally, future work should seek to understand whether there is an increase in mental workload with additional DOFs of haptic guidance.

ACKNOWLEDGMENT

TRI provided funds to assist the authors with their research, but this article solely reflects the opinions and conclusions of its authors and not TRI or any other Toyota entity.

REFERENCES

- [1] S. Kalyuga, *Instructional Guidance: A Cognitive Load Perspective*. Charlotte, NC, USA: Information Age Publishing, 2015.
- [2] A. Dey, M. Billingham, R. W. Lindeman, and J. E. Swan, "A systematic review of 10 years of augmented reality usability studies: 2005 to 2014," *Front. Robot. AI*, vol. 5, no. 37, pp. 1–28, 2018.
- [3] C. D. Wickens, "Multiple resources and mental workload," *Human Factors*, vol. 50, no. 3, pp. 449–455, 2008.
- [4] J. V. Hanson, D. Whitaker, and J. Heron, "Preferential processing of tactile events under conditions of divided attention," *NeuroReport*, vol. 20, no. 15, pp. 1392–1396, 2009.
- [5] L. Marchal-Crespo, M. van Raaij, G. Rauter, P. Wolf, and R. Riener, "The effect of haptic guidance and visual feedback on learning a complex tennis task," *Exp. Brain Res.*, vol. 231, no. 3, pp. 277–291, 2013.
- [6] B. A. Forsyth and K. E. MacLean, "Predictive haptic guidance: Intelligent user assistance for the control of dynamic tasks," *IEEE Trans. Vis. Comput. Graph.*, vol. 12, no. 1, pp. 103–113, Jan./Feb. 2006.
- [7] L. Marchal-Crespo and D. J. Reinkensmeyer, "Review of control strategies for robotic movement training after neurologic injury," *J. NeuroEngineering Rehabil.*, vol. 6, no. 1, 2009, Art. no. 20.
- [8] G. Grindlay, "Haptic guidance benefits musical motor learning," in *Proc. Symp. Haptic Interfaces Virtual Environment Teleoperator Syst.*, 2008, pp. 397–404.
- [9] J. Lee and S. Choi, "Effects of haptic guidance and disturbance on motor learning: Potential advantage of haptic disturbance," in *Proc. IEEE Haptics Symp.*, 2010, pp. 335–342.
- [10] J. J. Abbott, P. Marayong, and A. M. Okamura, "Haptic virtual fixtures for robot-assisted manipulation," *Springer Tracts Adv. Robot.*, vol. 28, pp. 49–64, 2007.
- [11] J. M. Walker, N. Zemiti, P. Poignet, and A. M. Okamura, "Holdable haptic device for 4-DOF motion guidance," in *Proc. IEEE World Haptics Conf.*, 2019, pp. 109–114.
- [12] S. A. Bowyer, B. L. Davies, and F. Rodriguez y Baena, "Active constraints/virtual fixtures: A survey," *IEEE Trans. Robot.*, vol. 30, no. 1, pp. 138–157, Feb. 2014.
- [13] M. K. O'Malley, A. Gupta, M. Gen, and Y. Li, "Shared control in haptic systems for performance enhancement and training," *ASME J. Dynamic Syst., Meas., Control*, vol. 128, pp. 75–85, 2006.
- [14] F. Hemmert, S. Hamann, M. Lowe, A. Wohllauf, J. Zeipelt, and G. Joost, "Take me by the hand: haptic compasses in mobile devices through shape change and weight shift," in *Proc. Nordic Conf. Human-Comput. Interaction*, 2010, pp. 671–674.
- [15] A. J. Spiers, J. van Der Linden, M. Oshodi, and A. M. Dollar, "Development and experimental validation of a minimalistic shape-changing haptic navigation device," in *Proc. IEEE Int. Conf. Robot. Autom.*, 2016, pp. 2688–2695.
- [16] M. Antolini, M. Bordegoni, and U. Cugini, "A haptic direction indicator using the gyro effect," in *Proc. IEEE World Haptics Conf.*, 2011, pp. 251–256.
- [17] J. M. Walker, H. Culbertson, M. Raitor, and A. M. Okamura, "Haptic orientation guidance using two parallel double-gimbal control moment gyroscopes," *IEEE Trans. Haptics*, vol. 11, no. 2, pp. 267–278, Apr.–Jun. 2018.
- [18] G. Jansson, "Tactile guidance of movement," *Int. J. Neuroscience*, vol. 19, no. 1–4, pp. 37–46, 1983.
- [19] S. Günther, F. Müller, M. Funk, J. Kirchner, N. Dezfuli, and M. Mühlhäuser, "TactileGlove: Assistive spatial guidance in 3D space through vibrotactile navigation," in *Proc. Conf. Pervasive Technol. Related Assistive Environments*, 2018, pp. 273–280.
- [20] H. Culbertson, J. M. Walker, M. Raitor, and A. M. Okamura, "WAVES: A wearable asymmetric vibration excitation system for presenting three-dimensional translation and rotation cues," in *Proc. ACM CHI Conf. Human Factors Comput. Syst.*, 2017, pp. 4972–4982.
- [21] T. Amemiya, T. Maeda, and H. Ando, "Location-free haptic interaction for large-area social applications," *Pers. Ubiquitous Comput.*, vol. 13, no. 5, pp. 379–386, 2009.
- [22] K. Bark, J. W. Wheeler, S. Premakumar, and M. R. Cutkosky, "Comparison of skin stretch and vibrotactile stimulation for feedback of proprioceptive information," in *Proc. Symp. Haptic Interfaces Virtual Environment Teleoperator Syst.*, 2008, pp. 71–78.
- [23] D. Prattichizzo, M. Otraduy, H. Kajimoto, and C. Pacchierotti, "Wearable and hand-held haptics," *IEEE Trans. Haptics*, vol. 12, no. 3, pp. 227–231, Jul.–Sep. 2019.
- [24] S. L. Norman, A. J. Doxon, B. T. Gleeson, and W. R. Provancher, "Planar hand motion guidance using fingertip skin-stretch feedback," *IEEE Trans. Haptics*, vol. 7, no. 2, pp. 121–130, Apr.–Jun. 2014.
- [25] F. Chinello, C. Pacchierotti, J. Bimbo, N. G. Tsagarakis, and D. Prattichizzo, "Design and evaluation of a wearable skin stretch device for haptic guidance," *IEEE Robot. Autom. Lett.*, vol. 3, no. 1, pp. 524–531, Jan. 2017.
- [26] A. L. Guinan, N. C. Hornbaker, M. N. Montandon, A. J. Doxon, and W. R. Provancher, "Back-to-back skin stretch feedback for communicating five degree-of-freedom direction cues," in *Proc. IEEE World Haptics Conf.*, 2013, pp. 13–18.
- [27] S. B. Schorr, Z. F. Quek, R. Y. Romano, I. Nisky, W. R. Provancher, and A. M. Okamura, "Sensory substitution via cutaneous skin stretch feedback," in *Proc. IEEE Int. Conf. Robot. Autom.*, 2013, pp. 2341–2346.
- [28] G. Campion, Q. Wang, and V. Hayward, "The Pantograph Mk-II: A haptic instrument," in *Proc. IEEE/RSJ Int. Conf. Intell. Robots Syst.*, 2005, pp. 723–728.
- [29] S. B. Schorr and A. M. Okamura, "Three-dimensional skin deformation as force substitution: Wearable device design and performance during haptic exploration of virtual environments," *IEEE Trans. Haptics*, vol. 10, no. 3, pp. 418–430, Jul.–Sep. 2017.
- [30] F. Conti *et al.*, "The CHAI Libraries," in *Proc. EuroHaptics Conf.*, 2003, pp. 496–500.
- [31] B. T. Gleeson, S. K. Horschel, and W. R. Provancher, "Design of a Fingertip-Mounted Tactile Display with Tangential Skin Displacement Feedback," *IEEE Trans. Haptics*, vol. 3, no. 4, pp. 297–301, Oct.–Dec. 2010.
- [32] S. Armstrong, M. V. Sale, and R. Cunningham, "Neural oscillations and the initiation of voluntary movement," *Frontiers Psychology*, vol. 9, 2018, Art. no. 2509.
- [33] K. Toohey and M. Duckham, "Trajectory similarity measures," *SIGSPATIAL Special*, vol. 7, no. 1, pp. 43–50, 2015.
- [34] J. Hong, L. Stearns, J. Froehlich, D. Ross, and L. Findlater, "Evaluating angular accuracy of wrist-based haptic directional guidance for hand movement," in *Proc. Graph. Interface*, 2016, pp. 195–200.
- [35] V. Van Polanen, W. M. Bergmann Tiest, and A. M. Kappers, "Movement strategies in a haptic search task," in *Proc. IEEE World Haptics Conf.*, 2011, pp. 275–280.
- [36] I. Birznieks, P. Jenmalm, a. W. Goodwin, and R. S. Johansson, "Encoding of direction of fingertip forces by human tactile afferents," *J. Neuroscience*, vol. 21, no. 20, pp. 8222–8237, 2001.